

## Stress Overshoot of Entangled Polymers in $\Theta$ Solvent

Tadashi Inoue,\* Yasuhiro Yamashita, and Hiroshi Watanabe

Institute for Chemical Research, Kyoto University,  
Uji, Kyoto 611-0011, Japan

Maya K. Endoh and Takeji Hashimoto

Department of Polymer Chemistry, Graduate School of  
Engineering, Kyoto University, Kyoto-Daigaku Katsura,  
Nishigyo-ku, Kyoto 615-8510, Japan

Received January 25, 2004

Revised Manuscript Received April 1, 2004

### Introduction

One of the important nonlinear viscoelastic features of polymeric liquids is the stress overshoot observed after start-up of fast shear.<sup>1</sup> For entangled polymer solutions in good solvents, the overshoot peak emerges at a constant strain  $\gamma_{\text{peak}} \cong 2$  for the shear stress and at  $\gamma_{\text{peak}} \cong 4$  for the first normal stress difference if the shear rate  $\dot{\gamma}$  is in the range of  $1/\tau_w \ll \dot{\gamma} \ll 1/(2\tau_R)$ , where  $\tau_w (= J_e\eta_0)$ ;  $J_e$  = steady-state compliance and  $\eta_0$  = zero-shear viscosity) is the terminal linear viscoelastic relaxation time and  $\tau_R$  is the longest viscoelastic Rouse relaxation time. Under faster shear at  $\dot{\gamma} \gg 1/(2\tau_R)$ , the stress overshoot peak is observed at a constant time,  $t_{\text{peak}} \cong 2\tau_R$ .<sup>2,3</sup> These features in good solvents (as well as in bulk) are well described with the modified tube theory incorporating a finite chain retraction time formulated by Pearson et al.<sup>3,4</sup> Thus, the stress overshoot in good solvents is well correlated to the chain retraction process having the characteristic time  $2\tau_R$ .

On the other hand, in  $\Theta$  solvents, viscoelastic properties of entangled polymers have not been completely understood yet. In a previous study, we compared linear viscoelastic behavior of entangled polystyrene (PS) chains of various molecular weights  $M$  in good and  $\Theta$  solvents.<sup>5</sup> The rubbery plateau modulus,  $G_N$ , was independent of  $M$  and did not change with the solvent quality. This result is contradicting to the original scaling theory by de Gennes<sup>6</sup> but can be explained with the modified scaling theory by Colby et al.,<sup>7</sup> who distinguished two length scales: the correlation length in concentration fluctuation and the two-points contact (entanglement) length. More importantly, the width (frequency/time span) of the rubbery plateau was found to be wider in the  $\Theta$  solvent than in the good solvent although the entanglement density,  $M/M_e$  with  $M_e$  being the molecular weight of an entanglement segment determined from  $G_N$ , was the same in these solvents. Furthermore, the terminal relaxation mode distribution was broader in the  $\Theta$  solvent.

The plateau width represents the  $\tau_w/\tau_e$  ratio, where  $\tau_e$  is the relaxation time of the entanglement segment. In the standard molecular picture, this ratio is believed to be a universal function of  $M/M_e$  and not directly dependent on the solvent quality, and the relaxation mode distribution is also believed to be universally

determined by the  $M/M_e$  ratio. Thus, the above differences of the DOP and TCP solutions having the same  $M/M_e$  ratio do not fit in this standard picture. We attributed these differences to the concentration fluctuation characteristic of the  $\Theta$  solution. According to the results of scattering experiments for semidilute polystyrene solutions in  $\Theta$  solvents, the correlation length of the concentration fluctuation,  $\xi$ , is comparable to the entanglement length scale,  $\xi_e$ , the latter being regarded as a tube diameter in the solutions.<sup>8</sup> Thus, some portions of the backbone of a given chain are in a less concentrated regime, and the other portions are in a more concentrated regime. For such chains, the large scale motion resulting in the terminal linear viscoelastic relaxation would be retarded by a magnitude determined by the motion in the most concentrated regime created by the fluctuation. (In other words, the fluctuation amplitude would determine this magnitude of retardation.)

In relation to this molecular interpretation, we expect that the chain retraction process governing the nonlinear overshoot phenomena is also affected by the concentration fluctuation. In this Note, we investigate the stress overshoot of entangled solutions in  $\Theta$  and good solvents to examine this expectation.

### Experimental Section

A high- $M$  polystyrene sample having a sharp molecular weight distribution, F550 ( $M_w = 5.5 \times 10^6$  and  $M_w/M_n = 1.15$ ; the supplier's designation), was purchased from Toso Co., Ltd. The good and  $\Theta$  solvents for F550, tricresyl phosphate (TCP), and dioctyl phthalate (DOP) were purchased from Waka Co. and used as supplied. The  $\Theta$  temperature of PS in DOP is 22 °C.<sup>5</sup>

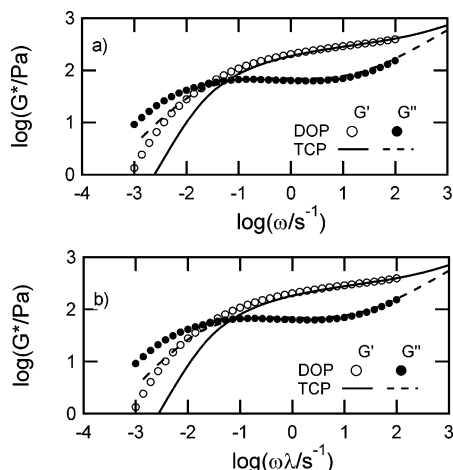
The storage and loss moduli,  $G'$  and  $G''$ , were measured with a laboratory rheometer (ARES, Rheometric Scientific) equipped with a cone-plate fixture of 25 mm diameter. The shear stress,  $\sigma$ , and the first normal stress difference,  $N_1$ , were measured with the same apparatus as functions of time,  $t$ , after the start-up of steady shear flow at various rates  $\dot{\gamma}$ . The precisions of the measurements of  $\sigma$  and  $N_1$  were  $\cong 0.5$  Pa and  $\cong 80$  Pa, respectively. The experiments were repeated from the scratch for freshly/separately prepared PS/DOP solutions for three times, and the reproducibility within this precision was confirmed.

### Results and Discussion

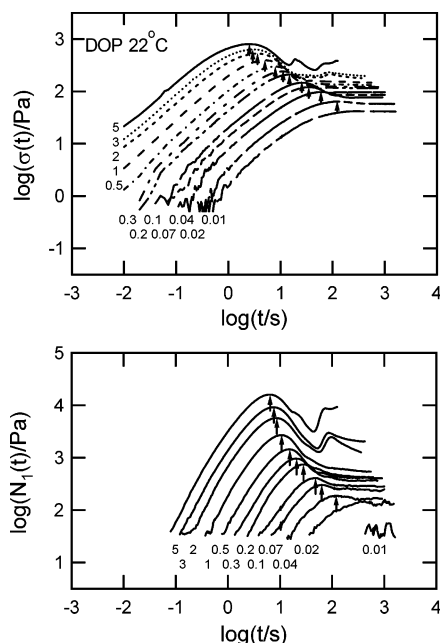
**Overview.** Figure 1a compares the angular frequency ( $\omega$ ) dependence of  $G'$  and  $G''$  for F550 in DOP and TCP at a concentration  $c = 0.0593$  g cm<sup>-3</sup> at the  $\Theta$  temperature in DOP,  $T = 22$  °C. Although not shown here, the data for the F550/TCP solution (obeying the time temperature superposition) were measured also in a higher  $\omega a_T$  regime where the Rouse-like  $\omega^{1/2}$  dependence of  $G'$  was observed.<sup>2</sup>

Figure 1a demonstrates that the rubbery plateau modulus,  $G_N$ , is the same in TCP and DOP (the good and  $\Theta$  solvents). However, the width of this plateau is larger in DOP, as clearly demonstrated in Figure 1b where the  $G'$  and  $G''$  curves of the F550/TCP solution are shifted along the  $\omega$  axis by a factor  $\lambda$  so that the  $G'$  data point of the F550/DOP solution at the highest  $\omega$  ( $= 10^2$  s<sup>-1</sup>) is superposed on the shifted TCP curve. This minor shift ( $\lambda = 1.2$ ) gives an excellent superposition of both  $G'$  and  $G''$  curves of the two solutions in a high- $\omega$

\* To whom all correspondence should be addressed. E-mail: tinoue@scl.kyoto-u.ac.jp.



**Figure 1.** Comparison of  $G^*$  of PS solutions in DOP ( $\Theta$ ) and TCP (good) at 22 °C ( $\Theta$  temperature in DOP); part a. In part b,  $G^*$  data for the PS/TCP solution are shifted along the frequency axis. This shift gives coincidence of the data of the two solutions at high frequencies.



**Figure 2.** Stress growth after start-up of steady shear observed for the PS/DOP solution at 22 °C. Numbers represent the shear rate  $\dot{\gamma}$  /s $^{-1}$ . Arrows indicate location of the stress peaks.

regime, indicating a coincidence of the measured low-frequency part of the fast viscoelastic mode distribution in the two solutions. This coincidence suggests that the local dynamics governing these modes are the same for these solutions in the shifted frequency scale. The difference in the rubbery plateau width, reflecting a difference in the terminal relaxation time normalized by a local friction, is quite clearly noted in this scale. These differences become smaller with increasing  $T$ , as discussed in more details in the previous paper.<sup>5</sup>

Figure 2 shows the growth of the shear stress  $\sigma$  and the first normal stress difference  $N_1$  of the F550/DOP solution after start-up of the shear flow at 22 °C. At low shear rates  $\dot{\gamma} < 0.02$  s $^{-1}$ , both  $\sigma$  and  $N_1$  monotonically increase with  $t$  and reach the steady state at  $t > 200$  s. At higher  $\dot{\gamma}$ , both  $\sigma$  and  $N_1$  exhibit the overshoot before reaching the steady state. The overshoot peak emerges at a shorter  $t$  on an increase of  $\dot{\gamma}$  up to 2 s $^{-1}$ , and the

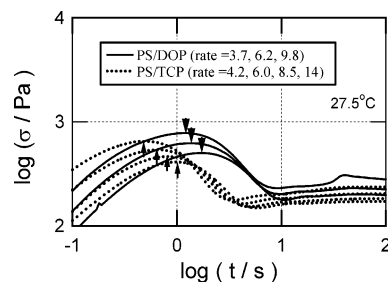


**Figure 3.** Comparison of the stress overshoot behavior of the PS/DOP and PS/TCP solutions at 27.5 °C.

peak time becomes insensitive to  $\dot{\gamma}$  for  $\dot{\gamma} > 2$  s $^{-1}$ . Similar behavior was observed in TCP.<sup>3</sup>

Kume et al.<sup>9,10</sup> showed that PS/DOP solutions of various  $M$  and  $c$  exhibit shear-induced phase separation in the steadily flowing state at  $\dot{\gamma} > 1/\tau_w$ . Indeed, we confirmed this phase separation in our F550/DOP solution ( $c = 0.0593$  g cm $^{-3}$ ) with naked eyes. One may suspect that the overshoot seen in Figure 2b may be related to the phase separation. However, for a F550/DOP solution at the same  $c$  prepared from the same commercial batch of F550, Kume et al.<sup>9,10</sup> observed significant light scattering (due to the phase separation) at 22 °C only at  $t$  longer than the overshoot peak time,  $t_{\text{peak}}$ . Thus, the  $t_{\text{peak}}$  itself appears to be hardly influenced by the shear-induced phase separation, although the evolution of  $\sigma$  and  $N_1$  at  $t > t_{\text{peak}}$  should be affected by this phase separation. (This evolution will be discussed together with the light scattering data in a future publication.) The lack of the effect of the phase separation on  $t_{\text{peak}}$  sounds reasonable because the phase separation should require large-scale motion of the chain corresponding to the terminal linear viscoelastic relaxation while the overshoot is governed by the *faster*, nonlinear chain retraction process occurring at  $t \ll \tau_w$ .

Figure 3 compares the overshoot behavior of the shear stress  $\sigma$  for the TCP and DOP solutions ( $c = 0.0593$  g cm $^{-3}$ ) at a higher  $T$ , 27.5 °C. The magnitude of the overshoot is similar for the TCP and DOP solutions, but  $t_{\text{peak}}$  is shorter for the former.

**Mechanism of Overshoot in Good and  $\Theta$  Solvents.** As described earlier, the stress overshoot features in good solvents can be well related to the chain retraction having the characteristic time  $2\tau_R$ , where  $\tau_R$  is the longest viscoelastic Rouse relaxation time at equilibrium (in the linear regime). The same molecular picture may hold also for  $\Theta$  solutions. However, the equilibrium  $\tau_R$  in the  $\Theta$  solutions may be affected by the concentration fluctuation therein, and a method of evaluating  $\tau_R$  is a quite important issue for understanding the overshoot features in those solutions, as explained below.

No significant concentration fluctuation exists in the PS solutions in the good solvent, TCP. For these solutions, the *standard* Rouse model assuming the same local friction and a uniform osmotic field along the chain backbone would be applicable, and the equilibrium  $\tau_R$  can be estimated with method of Osaki et al.<sup>2,3,11</sup> based on this model: They focused on the high- $\omega$  Rouse regime where  $G'$  was proportional to  $\omega^{1/2}$  and evaluated the equilibrium Rouse time as  $\tau_R^0 = \{aM/(1.11cRT)\}^2$ , where  $a$  is the  $G'/\omega^{1/2}$  ratio being independent of  $\omega$  in this regime and the numerical factor of 1.11 is obtained from the standard Rouse model. Thus, we applied their method to the high- $\omega$  data of our PS/TCP solution reported previously<sup>2</sup> to evaluate  $\tau_R^0$  of this solution (with

**Table 1. Characteristic Relaxation Times at 22 °C**

| solvent | $\tau_w/s$ | $\tau_R^\circ/s$ | $\tau_R^h/s$ | $\lambda'^a$ |
|---------|------------|------------------|--------------|--------------|
| DOP     | 140        | 0.29             | 0.94         | 1.6          |
| TCP     | 52         | 0.35             |              | 0.97         |

<sup>a</sup>  $\lambda' = \tau_R^{NL}/\tau_R^\circ$  in TCP and  $\lambda' = \tau_R^{NL}/\tau_R^h$  in DOP.

**Table 2. Characteristic Relaxation Times at 27.5 °C**

| solvent | $\tau_w/s$ | $\tau_R^\circ/s$ | $\tau_R^h/s$ | $\lambda'^a$ |
|---------|------------|------------------|--------------|--------------|
| DOP     | 78         | 0.18             | 0.52         | 1.2          |
| TCP     | 33         | 0.22             |              | 0.97         |

<sup>a</sup>  $\lambda' = \tau_R^{NL}/\tau_R^\circ$  in TCP and  $\lambda' = \tau_R^{NL}/\tau_R^h$  in DOP.

the superscript “o” standing for this specific method). The results are summarized in Tables 1 and 2.

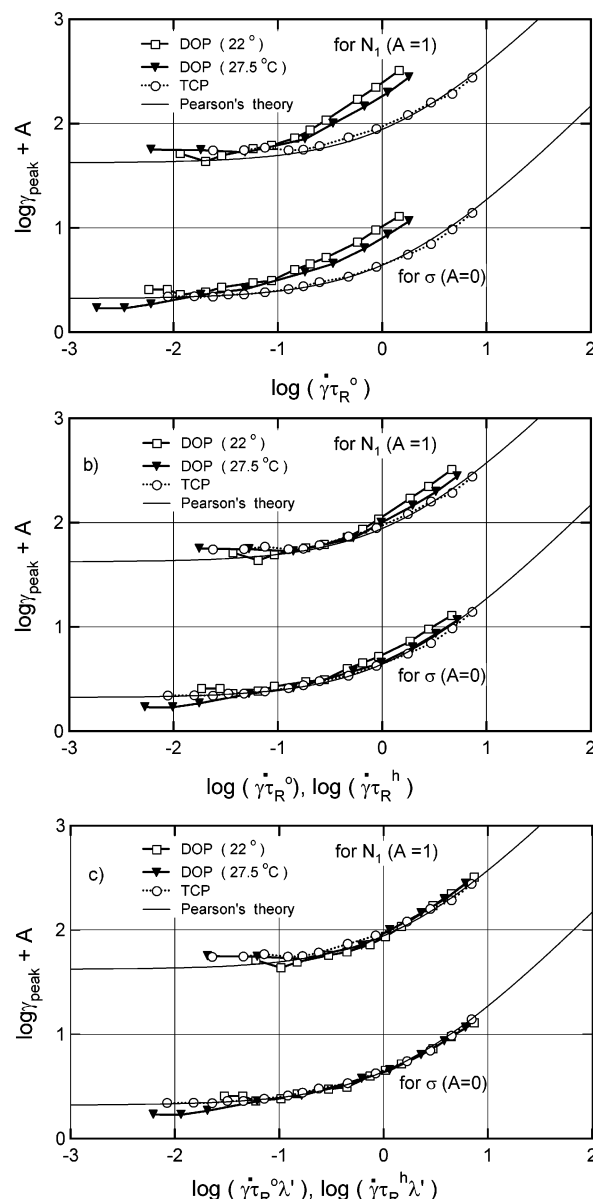
For the PS/DOP solutions at 22 and 27.5 °C, no Rouse regime is clearly observed in our experimental window (cf. Figure 1a). However, the  $G'$  and  $G''$  data of the DOP and TCP solutions in the shifted frequency scale (Figure 1b) are indistinguishable at high  $\omega$  where the TCP solution exhibits a crossover to the Rouse behavior ( $G' \propto \omega^{1/2}$ ). Thus, the  $\tau_R^\circ$  in the DOP solution defined on the basis of the standard Rouse model (and to be evaluated with the above method) can be estimated from  $\tau_R^\circ$  in the TCP solution;  $\tau_R^\circ(\text{DOP}) = \tau_R^\circ(\text{TCP})/\lambda$  with  $\lambda$  being the minor shift factor explained for Figure 1b. The  $\tau_R^\circ(\text{DOP})$  values thus determined are also summarized in Tables 1 and 2.

Figure 4a shows the strain at the overshoot peak of the DOP and TCP solutions,  $\gamma_{\text{peak}} = \dot{\gamma} t_{\text{peak}}$ , plotted against the normalized shear rate,  $\dot{\gamma} \tau_R^\circ$ . Clearly,  $\gamma_{\text{peak}}$  is constant ( $\approx 2$  for  $\sigma$  and  $\approx 4$  for  $N_1$ ) for both of the DOP and TCP solutions at the shear rates in a range of  $0.1/\tau_R^\circ > \dot{\gamma} (> 1/\tau_w)$ . Under faster shear,  $\gamma_{\text{peak}}$  increases with increasing  $\dot{\gamma}$ . For the TCP solution, the  $\gamma_{\text{peak}}$  data are in close agreement with the modified tube theory of Pearson et al.<sup>4</sup> shown with the thin solid curves. This agreement, also noted for PS/TCP solutions examined in a previous study,<sup>3</sup> strongly suggests that the nonlinear chain retraction resulting in the overshoot in the good solvent (TCP) is characterized with the equilibrium Rouse time  $\tau_R^\circ$  defined for the frictionally/osmotically uniform chain.

In contrast, the  $\gamma_{\text{peak}}$  of the DOP solution under fast shear is considerably larger than that of the TCP solution when plotted against  $\dot{\gamma} \tau_R^\circ$  and does not obey the tube theory utilizing the  $\tau_R^\circ$ . Thus, the effect of the solvent quality on the overshoot behavior is clearly noted under the fast shear. Indeed, an enhancement of the solubility of F550 in DOP with increasing  $T$  (from 22 to 27.5 °C) results in a decrease of  $\gamma_{\text{peak}}$  of the DOP solution toward  $\gamma_{\text{peak}}$  of the TCP solution.

The above difference between the DOP and TCP solutions under the fast shear may be related to the equilibrium concentration fluctuation in the former. In other words, the difference may have emerged because the  $\tau_R^\circ$  defined for the frictionally/osmotically uniform chain was utilized for the PS chain under the fluctuation created heterogeneities in the friction distribution and osmotic field. Thus, the overshoot in DOP and TCP may be commonly related to the Rouse-type retraction if the equilibrium Rouse time under these heterogeneities is appropriately evaluated for the PS chain in DOP.

In relation to this evaluation, we remember that the terminal relaxation of  $G^*$  is retarded in DOP possibly due to the heterogeneities in the friction distribution and osmotic field (cf. Figure 1b). In homogeneous



**Figure 4.** Shear rate dependence of the strains at the overshoot peaks of the shear stress and first normal stress difference. The dependence predicted by the modified tube model of Pearson et al. is shown with the thin solid curves.

solutions, the terminal relaxation time  $\tau_w$  and the Rouse relaxation time  $\tau_R$  are related as  $\tau_w = \tau_R(M/M_e)^\alpha$  with  $\alpha \approx 1.4$ .<sup>12</sup> Thus, we may assume that the difference between  $\tau_w$ 's of the PS/DOP and PS/TCP solutions having the same  $M/M_e$  value represents the difference between the equilibrium  $\tau_R$ 's of these solutions. Under this assumption, we estimated  $\tau_R$  in the DOP solution as  $\tau_R^h(\text{DOP}) = \tau_R^\circ(\text{TCP})\{\tau_w(\text{DOP})/\tau_w(\text{TCP})\}$ , with the superscript “h” standing for the heterogeneities considered in  $\tau_R^h$ . The  $\tau_R^h(\text{DOP})$  values thus obtained are summarized in Tables 1 and 2.

The heterogeneities would have just minor effects on local Rouse modes (thereby allowing the coincidence of the fast viscoelastic mode distribution in DOP and TCP; cf. Figure 1b) but significantly influence the global Rouse modes. The  $\tau_R^h(\text{DOP})$  characterizes such global modes at equilibrium. In Figure 4b,  $\gamma_{\text{peak}}$  of the PS/DOP solutions is plotted against the shear rate normalized by this equilibrium Rouse time,  $\dot{\gamma} \tau_R^h$ . This plot approximately agrees with the plot of  $\gamma_{\text{peak}}$  of the PS/TCP



solutions against the normalized shear rate  $\dot{\gamma}\tau_R^\circ$  considering no heterogeneities. This result suggests that the overshoot features in DOP are determined, to a considerable extent, by the equilibrium Rouse motion in the presence of the heterogeneities due to the concentration fluctuation.

At the same time, a small but nonnegligible difference is noted between the plots for the PS/DOP and PS/TCP solutions in Figure 4b. In relation to this difference, we note that a relative change of  $\gamma_{\text{peak}}$  with  $\dot{\gamma}$  is quite similar in these solutions. Indeed, the  $\gamma_{\text{peak}}$  curves of both DOP and TCP solutions can be excellently superposed on the theoretical curve after horizontal shifts by respective factors  $\lambda'$ , as shown in Figure 4c. The  $\lambda'$  values are summarized in Tables 1 and 2.

The validity of this horizontal shift strongly suggests that an *effective* chain retraction time governing the nonlinear overshoot,  $\tau_R^{\text{NL}}$ , is larger than  $\tau_R^\circ$  (TCP) and/or  $\tau_R^{\text{h}}$  (DOP) by the factor  $\lambda'$ .  $\lambda'$  is close to unity in TCP but moderately larger than unity in DOP; see Tables 1 and 2. This result suggests that the chain retraction in TCP is governed by the equilibrium Rouse dynamics in the absence of heterogeneities while the retraction dynamics in DOP is influenced also by the shear. This shear effect in DOP may be attributed to a shear-induced enhancement of the concentration fluctuation in DOP. (This enhancement can be interpreted as a pretransition effect of the shear-induced phase separation occurring at  $t \gg t_{\text{peak}}$  and  $\dot{\gamma} \gg \dot{\gamma}_{\text{peak}}$ .)

In summary, the analysis in Figure 4a–c suggests that the nonlinear overshoot features in the  $\Theta$  solvent (DOP) related to the chain retraction are determined, to a considerable extent, by the equilibrium Rouse motion in the presence of the heterogeneities due to the concentration fluctuation. At the same time, the shear-induced enhancement of the fluctuation may also have some effect on those features. In contrast, in the good solvent (TCP), the overshoot features appear to be governed by the equilibrium Rouse motion in the absence of the heterogeneities, and the mechanism of the chain retraction itself seems to be hardly affected by the shear.

### Concluding Remarks

The stress overshoots in the  $\Theta$  and good solvents are commonly governed by the nonlinear chain retraction process. However, the retraction in the  $\Theta$  solvent is significantly retarded compared to that in the good

solvent, as is the case also for the equilibrium chain motion corresponding to the linear viscoelastic terminal relaxation in these solvents. The molecular origin of this retardation appears to be the significant concentration fluctuation in the  $\Theta$  solutions that already exists at equilibrium and is possibly enhanced to some extent under the shear.

### References and Notes

- (1) Graessley, W. W. *Adv. Polym. Sci.* **1974**, *16*, 1.
- (2) Osaki, K.; Inoue, T.; Uematsu, T.; Yamashita, Y. *J. Polym. Sci., Polym. Phys. Ed.* **2001**, *39*, 1704.
- (3) Osaki, K.; Inoue, T.; Isomura, T. *J. Polym. Sci., Polym. Phys. Ed.* **2000**, *38*, 1917.
- (4) Pearson, D.; Herbolzheimer, E.; Grizzuti, N.; Marrucci, G. *J. Polym. Sci., Polym. Phys.* **1991**, *29*, 1589.
- (5) Inoue, T.; Yamashita, Y.; Osaki, K. *Macromolecules* **2002**, *35*, 9169.
- (6) de Gennes, P.-G. *Scaling Concepts in Polymer Physics*; Cornell University Press: Ithaca, NY, 1979.
- (7) Colby, R. H.; Rubinstein, M. *Macromolecules* **1990**, *23*, 2753.
- (8) (a) For semidilute polystyrene solutions, empirical equations have been reported for the correlation length of the concentration fluctuation  $\xi$  and the entanglement length scale  $\xi_e$ :  $\xi = 5.5 \times 10^{-8} c^{-1}$  cm in  $\Theta$  solvents<sup>8b–d</sup> and  $\xi_e = 3.11 \times 10^{-7} c^{-0.7}$  cm in good solvents,<sup>8e</sup> where  $c$  is the concentration in units of g cm<sup>-3</sup>. Since  $G_N$  corresponding to  $\xi_e$  is insensitive to solvent quality (see Figure 1), we may apply the latter equation also to  $\Theta$  solutions. For the polystyrene solution in DOP examined in this paper ( $c = 0.0593$  g cm<sup>-3</sup>), these equations give comparable values of the two length scales,  $\xi = 0.93 \times 10^{-6}$  cm and  $\xi_e = 2.2 \times 10^{-6}$  cm. (b) Cotton, J. P.; Nierlich, M.; Boue, F.; Daoud, M.; Farnoux, B.; Jannink, G.; Duplessiz, R.; Picot, C. *J. Chem. Phys.* **1976**, *65*, 1101. (c) Stepanek, P.; Perzyunski, R.; Delsanti, M.; Adam, M. *Macromolecules* **1984**, *17*, 2340. (d) Adam, M.; Delsanti, M. *Macromolecules* **1985**, *18*, 1760. (e) Nemoto, N.; Makita, Y.; Tsunashima, Y.; Kurata, M. *Macromolecules* **1984**, *17*, 2629.
- (9) Kume, T.; Hashimoto, T.; Takahashi, T.; Fuller, G. B. *Macromolecules* **1997**, *30*, 7232.
- (10) Kume, T.; Hattori, T.; Hashimoto, T. *Macromolecules* **1997**, *30*, 427.
- (11) Inoue, T.; Yamashita, Y.; Osaki, K. *Macromolecules* **2002**, *35*, 4718.
- (12) (a) The empirical relationship for homogeneous solutions,  $\tau_w = \tau_R(M/M_e)^\alpha$  with  $\alpha \approx 1.4$ , can be deduced from the Doi model<sup>12b</sup> considering reptation and contour length fluctuation (CLF),  $\tau_{\text{rep}}^{(f)} \approx \tau_{\text{rep}} Q$  with  $\tau_{\text{rep}} \sim M^2/M_e$  being the reptation time without CLF and  $Q = [1 - 1.47(M/M_e)^{-1/2}]^2$ . The  $M$  dependence of this  $\tau_{\text{rep}}^{(f)}$  is approximated as  $M^{1.4}$  in a wide range of  $M$ , meaning that the  $Q$  factor is approximately proportional to  $(M/M_e)^{0.4}$  and thus  $\tau_{\text{rep}}^{(f)}$  scales as  $M^{1.4}/M_e^{1.4} \sim \tau_R(M/M_e)^{1.4}$ . (b) Doi, M. *J. Polym. Sci., Polym. Phys. Ed.* **1983**, *21*, 667.

MA049833Q